HHS Public Access

Author manuscript

Anal Chem. Author manuscript; available in PMC 2020 January 30.

Published in final edited form as:

Anal Chem. 2019 September 17; 91(18): 11872–11878. doi:10.1021/acs.analchem.9b02630.

Ultra-sensitive detection of human chorionic gonadotropin using frequency locked microtoroid optical resonators

Erol Ozgur[1], **Kara Ellen Roberts**[1], **Ekin Ozge Ozgur**[1], **Adley Nathanael Gin**[2], **Jaden Robert Bankhead**[2], **Zhikun Wang**[2], **Judith Su**[1,2,*]

[1]Department of Biomedical Engineering, University of Arizona, Tucson, AZ, 85721 USA

[2]College of Optical Sciences, University of Arizona, Tucson, AZ, 85721 USA

Abstract

Clean sport competition is of significant concern to many governments and sporting organizations. Highly sensitive and rapid sensors are needed to improve the detection of performance enhancing drugs in sports as athletes take diuretics to dilute the concentration of drugs in their urine and microdose under the detectable limits of current sensors. Here we demonstrate, using frequency locked microtoroid optical resonators, a three order of magnitude improvement in detection limit over the current gold standard, mass spectrometry, for the common performance enhancing drug, human chorionic gonadotropin (hCG). hCG, also known as the pregnancy hormone, was detected both in simulated urine and in the urine of pregnant donors at a concentration of 1 and 3 femtomolar, respectively. We anticipate that the sensitivity provided by frequency locked optical microcavities can enable a new standard in anti-doping research.

The use of performance enhancing drugs during athletic events is prohibited by the World Anti-Doping Association (WADA). To monitor the use of these drugs, anti-doping drug tests are routinely performed during athletic events[1,2]. These tests can detect minute quantities of chemicals from bodily fluids, such as blood or urine. Mass spectrometry is currently the gold standard[3,4] for detecting various doping agents; however, it can have insufficient limits of detection[5], requires a trained operator, involves specialized enzymes,[6,7] and can be expensive, costing in excess of 100 dollars per assay.

In this work we focus on detecting human chorionic gonadotropin (hCG) (Fig. 1a). hCG is a hormone secreted during pregnancy and is one of the most common doping agents[8]. It is used by athletes to increase the secretion of testosterone and is on the World Anti-Doping Association (WADA)'s list of prohibited substances for male athletes.[9] The smallest

* judy@optics.arizona.edu.

Author Contributions

JS conceived the idea. EO and JS designed the experiments. EO, KER, EOO, and AG prepared samples and took data. EOO and KER measured the hCG concentration in urine samples using pregnancy test strips. EO, KER, and EOO analysed the data. EO and ANG fabricated the microtoroids. JRB contributed to building the optical measurement system. ZW devised the temperature measurement setup and helped in measurements. EO, KER, and JS wrote the manuscript. All authors have read and commented on the manuscript.

Associated Content

Supplementary figures and additional results and discussion (PDF).

Competing Interests

J.S. owns a financial interest in Femtoray Technologies which specializes in molecular label-free sensors.

detectable quantity of hCG by mass spectrometry is approximately 2 pM[8], which is only slightly below the current doping threshold of 13 pM that has been imposed by WADA[10]. Based on the concentration of hCG measured in baseline samples of healthy male urine, it has been recommended to reduce the doping threshold further to ~ 2.4 pM in order to avoid false negative results in doping tests[2,5]. As mass spectrometry's limit of detection is very close to this level, it is unlikely that mass spectroscopy would be a robust and reliable method of enforcing this limit.

Because of its implications in pregnancy and doping, there has been much research done in enabling the sensitive and selective detection of hCG from bodily fluids[11]. The most effective techniques are either electrochemical or optical label-free biosensors.[11] Electrochemical sensors measure changes in electrical impedance when hCG binds to the sensor[12–19]. Although they have high sensitivities and in some cases can detect hCG at a concentration of 30 fM[17], electrochemical sensors can have issues with sample reproducibility and sensor stability.[20] Optical biosensors measure changes in absorption, refractive index, or light emission caused by analyte binding. These sensors typically rely on interferometry[21], surface plasmon resonance[22,23], photoluminescence[24–27], or electrochemiluminescence[18]. These existing optical techniques are, however, less sensitive than mass spectrometry[13–15,21–24] and require multiple steps which can increase user error. High-sensitivity single molecule optical biosensors have previously been demonstrated using optical microspheres coupled to plasmonic nanoparticles[28,29], but the effective active area of these sensors is very small, limited to just the locations of the plasmonic hot spots on the nanoparticles. In addition, these hybrid whispering gallery mode plasmonic sensors suffer from inconsistent signal amplification due to variations in size of the plasmonic particles. Whispering gallery mode microtoroid optical resonators have also been used to sense temperature changes[30] and particles in air[31].

Here, we report for the first time the use of a label-free optical biosensing scheme known as FLOWER (frequency locked optical whispering evanescent resonator)[32] to detect hCG in urine at a concentration as low as one femtomolar. This value is three orders of magnitude better than the capabilities of mass spectrometry. While we have previously reported using FLOWER to sense single macromolecules, this is the first demonstration of FLOWER for biodetection from human derived samples.

FLOWER uses optical whispering gallery mode technology in combination with electronic feedback control and data processing techniques to improve its signal-to-noise ratio. This enables thousands of times greater particle capture area than is provided by plasmonic particles, thus increasing the likelihood of detectable particle binding events. In general, optical microcavities such as microtoroids exhibit high detection sensitivity due to their long (on the order of tens of nanoseconds) photon confinement times. Each time light circulates the periphery of the resonator, it re-interrogates a bound analyte (Fig. 1b), causing large signal amplification. Particle binding events are detected by changes in the resonance frequency of the resonator due to changes in the refractive index within the evanescent field of the sensor. Functionalization of the sensor's surface using capture agents such as antibodies enables selective detection.

In standard biological sensing experiments using optical microcavities, changes in resonance frequency of the optical microcavity are tracked by continuously scanning the wavelength of a tunable laser. FLOWER is different in that it adaptively tracks the resonance frequency of the resonator as particles bind, enabling ultra-high sensitivity without requiring comparatively slow spectral scanning. Data acquisition rates on the order of several hundred kHz are possible, allowing the detection of fast events such as single particle binding[32] (Fig. 1c, see Methodology for details).

Methodology

Microtoroid fabrication.

Microtoroids were fabricated as previously described.[33] Briefly, circular pads of photoresist were patterned on silicon wafers with a 2 μm thick thermal oxide layer. The areas that were not protected by the photoresist were removed using a weak hydrofluoric acid etch. Silicon pillars were selectively dry etched using XeF_2, creating a microdisk structure. Afterwards, these structures were reflowed using a CO_2 laser. Light from a ~780 nm tunable laser was evanescently coupled into the microtoroids using a tapered optical fiber. The quality factors (Q) of the microtoroids were measured before each experiment. As higher Q-factors provide better limits of detection, only toroids with Q-values higher than 10^7 were used for these experiments. A Q of 10^7 can be reliably obtained whereas an order of magnitude higher in Q (10^8) is more rare. Typically, we achieve Q-factors on chip which range from 10^5–10^8.

Microtoroid functionalization.

Microtoroids were functionalized immediately after the CO_2 laser reflow process. Toroids were first incubated with a custom synthesized silane-PEG-maleimide linker solution for 30 min.[32] After linker incubation, the chips were rinsed with ultrapure water, and soaked in a 5 μg/ml solution of mouse monoclonal anti-hCG IgG antibody in Phosphate Buffered Saline (PBS) for 5 minutes. After another rinse with ultrapure water, the samples were mounted on the measurement stage using cyanoacrylate glue. The antibody-coated microtoroid was continually immersed in 100 μl of simulated urine (Carolina Biological Supply Company). According to the supplier's specifications, simulated urine is composed of 92.33% water, 7.64% glycerol, and 0.03% sodium hydroxide.

Experimental procedure.

A microaquarium was formed by gluing a glass coverslip to a glass spacer which was glued to the surface of our sample stage. The coverslips were pre-cleaned with 2-propanol and ultrapure water. All dilutions of hCG were prepared using simulated urine, except in the case of the bare microtoroid experiments, where sample dilutions were prepared using PBS. The laser frequency was locked to a resonance of microtoroid optical microcavity using a Toptica Digilock 110 frequency locking system, as previously described[34]. Cavity resonances were locked using a 2 kHz sinusoidal dither signal with a modulation amplitude of 15 mV. This corresponds to a dithering of 300 fm. Proportional-Integral-Derivative (PID) parameters were on the order of 10, 100, and 1, respectively, while an overall system gain on the order of 1000 was used. These parameters were slightly tuned in different experiments to obtain best results. Tuning was performed by applying a 0.1 V square voltage pulse at 0.5 Hz

frequency to modulate the wavelength and observing successful tracking of wavelength shifts. Data was recorded using a 24-bit data acquisition card. Concentration dependent data is obtained by directly increasing the analyte concentration without a washing step. The infusion of the analyte was performed using a peristaltic pump operating at a rate of 10 μl/s. The sample chamber volume is approximately 100 μl. The sample chamber was flushed with 300 μl of analyte containing solution to ensure that the fluid in the sample chamber has been completely exchanged. There is no separate rinsing step following exposure to analyte as this would increase experimental complexity and was not found to mitigate non-specific binding. After waiting for 30 s for fluid-driven fluctuations of the optical fiber to stop, the resonant wavelength is tracked. Data was recorded with an acquisition rate of 10 kHz. The silicone tubing used to inject analyte solutions was cleaned with 0.1 M HCl and subsequent diH_2O infusion before each experiment.

Data analysis.

Data was analysed using a custom MATLAB script. Resonant shifts were tracked over 20 seconds, which is long enough such that transients due to temperature and fiber taper fluctuations are less significant than binding-induced shifts, while keeping the total experiment time as short as possible, which is important for future high-throughput screening applications. After converting from voltage to wavelength (Fig. S2a), data was first Fourier filtered to remove 60 Hz electronic line noise and other periodic noise. (Fig. S2b and S2c). Then, a median filter of 1000 points was applied to smooth the data (Fig. S2d). The background noise level is measured as 0.0217 +/− 0.0069 fm at 1 s, and 0.0002 +/− 0.0001 fm at 1 ms, after Fourier and median filtering. The thermal drift was removed by subtracting a straight line corresponding to the initial slope of the filtered signal, since the thermal drifts in the relatively short measurement interval can be considered as linear. This assumption was verified by simultaneous temperature and wavelength shift measurements (Fig. S3 and Fig. S4).

Pregnancy test strip hCG concentration measurement.

Purified hCG, real urine samples obtained from pregnant donors at different trimesters of pregnancy, and control urine samples were each diluted in simulated urine. These samples were obtained commercially from Lee Biosolutions. Samples were diluted by factors of 10^2–10^6 to prevent saturation of the commercial test strips, which were used to quantify the amount of hCG from the pregnant donor samples. The images of test strips were collected using a smartphone camera under identical illumination conditions. The images were separated into their colour channels using ImageJ software and the green channel was used for analysis. After the selected channel was converted to grayscale and inverted, the average intensity from test line (T), control line (C), and background (B) were measured. The test line contrast is represented as:

$$\frac{T - B}{C - B}$$

Temperature measurements.

For measuring the correlation between temperature and resonance wavelength shifts of the microtoroid, a PID temperature controller was used to heat the sample stage. The temperature was simultaneously measured using a thermocouple. The cooling of the microtoroid was monitored within the time scale of the optical measurement and compared with the associated wavelength shift (Fig. S3). The data acquisition rate in thermal measurements was 1 Hz.

Results and Discussion

Limit of Detection of FLOWER for hCG

To determine the sensitivity of FLOWER for hCG detection, we measured the resonance frequency shifts associated with flowing different concentrations of hCG ranging from 100 aM to 10 nM over the toroid's surface (Fig. 2a). The same microtoroid was used for each curve in this dilution series. These experiments were repeated using two additional toroids (Fig. 2b). For selectivity purposes, experiments were performed using a microtoroid functionalized with monoclonal antibodies for hCG. Simulated urine, which is a mixture of water, glycerol, and sodium hydroxide and has the same pH as urine[35], was used to dilute the samples. The results demonstrate that our sensor can detect hCG over a 6 order of magnitude concentration range. The limit of detection was calculated to be 120 aM using the three-sigma method, which equals three times the standard deviation (σ) of repeated blank infusion experiments. The limit of quantification[36] which determines how well one can distinguish between two separate concentrations is defined as 10σ and is calculated here to be 400 aM. The lowest experimentally-detected concentration we measured in our experiments was 1 fM. A control experiment using anti-amyloid-β to which hCG is not expected to bind was also performed. In this case, no concentration dependent increase in binding was observed (Figure 2c). The individual binding curves for Fig. 2a are shown in Fig 2d.

We note that in these experiments, the binding response includes both a contribution from temperature as well as a hCG binding. In contrast, in single particle binding experiments[32], temperature drift occurs on a different time scale than particle binding. In addition, for single particle experiments, PID parameters were optimized for fast and small events. For the experiments in the current paper, which involve many molecules, the PID parameters are optimized to obtain a smooth curve without steps and the temperature drift is controlled by subtracting its contribution to the shift (Fig S4).

Measurement of hCG Levels in Urine

Using the calibration curve created from known concentrations of hCG spiked in simulated urine (Fig. 2), we used FLOWER to measure the concentration of hCG in real urine samples. As we did not have access to urine from athletes who dope with hCG, we instead measured the urine hCG levels obtained from pregnant women at different trimesters of pregnancy. As shown in Figure 3, we are able to detect hCG concentrations as low as 3 fM in human samples (Fig. 3b) diluted in simulated urine by a factor of 10^6. As control experiments, samples obtained from male and non-pregnant female urine samples were also diluted and

measured. There was no detectable concentration dependence in the rate of resonance wavelength shift at dilutions of 10^4 and 10^6 (Fig. 3e and 3f). This agrees with our expectations, as *undiluted* male and non-pregnant female urine typically contain approximately 120 and 150 fM hCG[37], respectively, and therefore, after dilution levels of 10^4 or 10^6, these concentrations would be below our detection threshold. Dilution also affects the concentrations of the other constituents in the urine and therefore also impacts nonspecific binding. For further validation, we also compared our FLOWER measurements of hCG to those of commercial pregnancy test strips (Fig. 3d and Fig. S1). The contrast of the test strip lines was calibrated with experiments performed using pregnancy test strips with known concentrations of hCG spiked into simulated urine (See Methods for details). Using the test strips, the hCG concentration for each trimester was measured to be 37 nM, 3 nM, and 11 nM, respectively. These values agreed well with our FLOWER measurements (Fig. 3d) and are within the reported range for hCG values during each trimester of pregnancy[38,39]; In addition, the relative amounts of hCG for each trimester are consistent with reported literature values, which indicate that hCG concentration is highest during the first trimester, is reduced tenfold during the second trimester, and reaches one half or one third the value of the first trimester during the third trimester.

Conclusions

We have demonstrated the detection of hCG in urine at a concentration of 1 fM in simulated urine and 3 fM in real urine samples. Our approach can provide high signal-to-noise ratio measurements over a large dynamic range. Figure 4 shows the limit of detection and the actual detection range of FLOWER in comparison with other hCG detection techniques, including mass spectrometry, which is the current gold standard. As shown in Figure 4, there is only one other technique, electrochemiluminescence[18], that claims a lower 3σ limit of detection; however, the actual lowest concentration measured in that study is still higher than what FLOWER can measure. In addition, FLOWER possesses a greater dynamic range. Furthermore, FLOWER does not require labeling of the target molecule, thus eliminating the need for fluorescent or radioactive tags which increase assay complexity and cost. With FLOWER, there is no need to vaporize samples as is done in gas chromatography mass spectrometry (GC-MS) and there is no need to pre-concentrate samples. For doping tests, as urine composition will be different for everyone, we would measure a baseline response from each athlete and use that value as a reference. In the future, we will employ alternative light coupling strategies so that a tapered optical fiber no longer needs to be used and these devices can be eventually manufactured and maintained at a user facility. As one example, we have recently demonstrated through simulation that nanoantennas can be used for robust free-space coupling of light into and out of these cavities.[40]

In conclusion, we have demonstrated a label-free method that has the potential to be widely used in doping detection. We anticipate that FLOWER has outstanding potential for preventing unethical conduct in sports by reducing false positives and negatives and by making tighter doping regulations enforceable.

Supplementary Material

Refer to Web version on PubMed Central for supplementary material.

Acknowledgements

This work was supported by the Partnership for Clean Competition Grant No. 2016R2000218G. The authors thank J. N. Wycoff for assistance in data collection.

References

(1). Butch AW; Woldemariam GA Drug Test. Anal 2016, 8, 1147–1151. [PubMed: 27594536]

(2). Butch AW; D AB; Avliyakulov NK Drug Test. Anal 2017.

(3). Thevis M; Thomas A; Schanzer W Anal. Bioanal. Chem 2011, 401, 405–420. [PubMed: 21424519]

(4). Krone N; Hughes BA; Lavery GG; Stewart PM; Arlt W; Shackleton CH The Journal of steroid biochemistry and molecular biology 2010, 121, 496–504. [PubMed: 20417277]

(5). Butch AW; D AB; Avliyakulov NK Drug Test. Anal 2017.

(6). Gundry RL; White MY; Murray CI; Kane LA; Fu Q; Stanley BA; Van Eyk JE Current protocols in molecular biology 2009, Chapter 10, Unit10 25.

(7). Giansanti P; Tsiatsiani L; Low TY; Heck AJR Nat. Protoc 2016, 11, 993–1006. [PubMed: 27123950]

(8). Woldemariam GA; Butch AW Clin. Chem 2014, 60, 1089–1097. [PubMed: 24899693]

(9). Thevis M; Kuuranne T; Geyer H Drug Test Anal 2018, 10, 9–27. [PubMed: 29149502]

(10). van den Broek I; Blokland M; Nessen MA; Sterk S Mass Spectrom. Rev 2015, 34, 571–594. [PubMed: 24375671]

(11). Fan J; Wang M; Wang CY; Cao Y Bioanalysis 2017, 9, 1509–1529. [PubMed: 29056064]

(12). Yang HC; Yuan R; Chai YQ; Su HL; Zhuo Y; Jiang W; Song ZJ Electrochim. Acta 2011, 56, 1973–1980.

(13). Sanchez S; Roldan M; Perez S; Fabregas E Anal. Chem 2008, 80, 6508–6514. [PubMed: 18662016]

(14). Teixeira S; Burwell G; Castaing A; Gonzalez D; Conlan RS; Guy OJ Sens. Actuator B-Chem 2014, 190, 723–729.

(15). Xia N; Chen ZH; Liu YD; Ren HZ; Liu L Sens. Actuator B-Chem 2017, 243, 784–791.

(16). Yang L; Zhao H; Fan SM; Deng SS; Lv Q; Lin J; Li CP Biosens. Bioelectron 2014, 57, 199–206. [PubMed: 24583692]

(17). Lu JJ; Liu SQ; Ge SG; Yan M; Yu JH; Hu XT Biosens. Bioelectron 2012, 33, 29–35. [PubMed: 22265320]

(18). Zhang A; Guo WW; Ke H; Zhang X; Zhang H; Huang CS; Yang DP; Jia NQ; Cui DX Biosens. Bioelectron 2018, 101, 219–226. [PubMed: 29096359]

(19). Yang H; Yuan R; Chai Y; Zhuo Y Colloids and surfaces. B, Biointerfaces 2011, 82, 463–469. [PubMed: 21030221]

(20). Stulik K Electroanal 1999, 11, 1001–1004.

(21). Schneider BH; Edwards JG; Hartman NF Clin. Chem 1997, 43, 1757–1763. [PubMed: 9299972]

(22). Boozer C; Yu QM; Chen SF; Lee CY; Homola J; Yee SS; Jiang SY Sens. Actuator B-Chem 2003, 90, 22–30.

(23). Dostalek J; Ctyroky J; Homola J; Brynda E; Skalsky M; Nekvindova P; Spirkova J; Skvor J; Schrofel J Sens. Actuator B-Chem 2001, 76, 8–12.

(24). Yan X; Huang ZB; He M; Liao XM; Zhang CQ; Yin GF; Gu JW Colloid Surf. B-Biointerfaces 2012, 89, 86–92.

(25). Zhou CH; Yuan H; Shen HB; Guo Y; Li XM; Liu D; Xu L; Ma L; Li LS J. Mater. Chem 2011, 21, 7393–7400.

(26). Wang WG; Zou YK; Yan JW; Liu J; Chen HX; Li S; Zhang L Spectroc. Acta Pt. A-Molec. Biomolec. Spectr 2018, 193, 102–108.

(27). Kuo HT; Yeh JZ; Jiang CM; Wu MC J. Immunol. Methods 2012, 381, 32–40. [PubMed: 22542932]

(28). Baaske MD; Foreman MR; Vollmer F Nat. Nanotechnol 2014, 9, 933–939. [PubMed: 25173831]

(29). Kim E; Baaske MD; Schuldes I; Wilsch PS; Vollmer F Science advances 2017, 3, e1603044. [PubMed: 28435868]

(30). Xu X; Chen W; Zhao G; Li Y; Lu C; Yang L Light, science & applications 2018, 7, 62.

(31). Zhu J; Ozdemir SK; Xiao Y-F; Li L; He L; Chen D-R; Yang L Nature Photonics 2009, 4, 46.

(32). Su J; Goldberg AFG; Stoltz BM Light Sci. Appl 2016, 5.

(33). Armani DK; Kippenberg TJ; Spillane SM; Vahala KJ Nature 2003, 421, 925–928. [PubMed: 12606995]

(34). Su J ACS Photonics 2015, 2, 1241–1245.

(35). Hamorsky KT; Ensor CM; Pasini P; Daunert S Anal. Biochem 2012, 421, 172–180. [PubMed: 22067979]

(36). Anal. Chem 1980, 52, 2242–2249.

(37). Stenman UH; Alfthan H; Ranta T; Vartiainen E; Jalkanen J; Seppala MJ Clin. Endocrinol. Metab 1987, 64, 730–736.

(38). MacGregor WG; Gale CW; Simmons E; Knight GJ J. Obstet. Gynaec. Brit. Cwlth 1966, 73, 775–782.

(39). Faiman C; Ryan RJ; Zwirek SJ; Rubin ME J. Clin. Endocrinol. Metab 1968, 28, 1323–1329. [PubMed: 5679995]

(40). Chen L, Li C, Su J, McLeod E Photonics Research 2019, 7, 967–976.

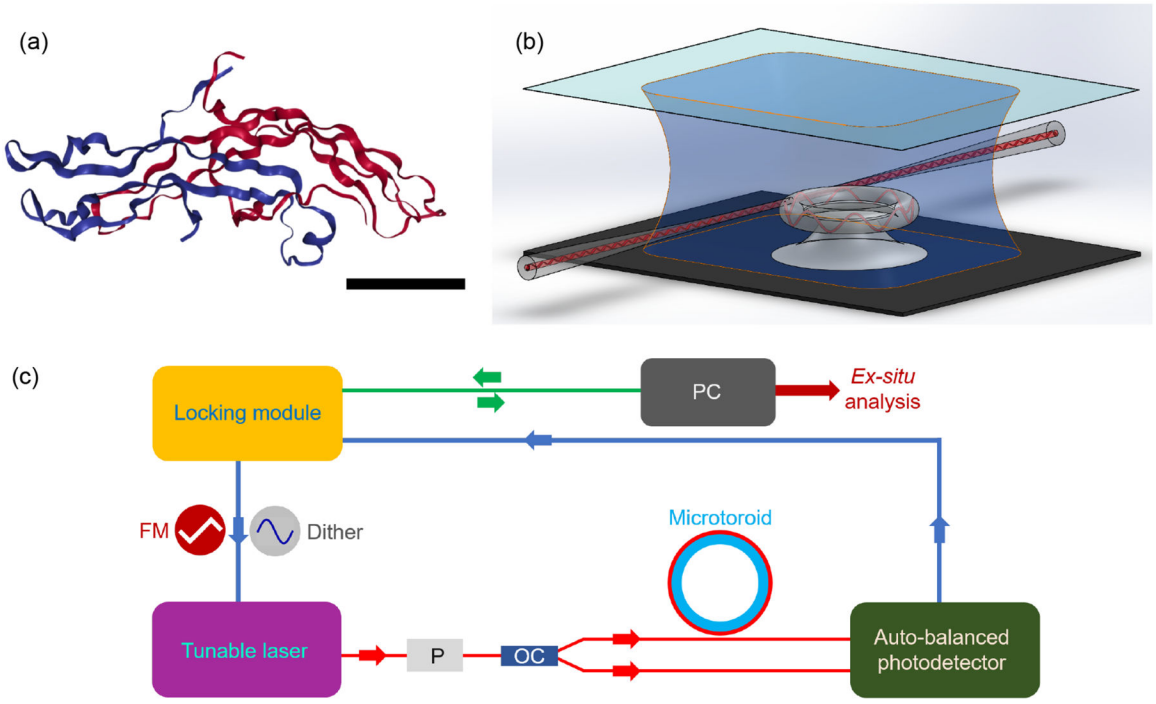

Fig. 1. High sensitivity optical biodetection using frequency locked microresonators.

(a) 3D structure of hCG, which is a 37.5 kDa protein, consisting of two subunits, α (blue) and β (red). The scale bar is 2 nm. (Image from the RCSB PDB (www.rcsb.org) of PDB ID 1HRP (Lapthorn, A.J., Harris, D.C., Littlejohn, A., Lustbader, J.W., Canfield, R.E., Machin, K.J., Morgan, F.J., Isaacs, N.W.) (1994) Crystal structure of human chorionic gonadotropin, *Nature* 369: 455–461) (b) Schematic of microtoroid resonator inside sample chamber. Light is evanescently coupled into a microtoroid using a tapered optical fiber. Analyte-containing solutions are flowed over the microtoroid sensor using a syringe pump. Binding of analyte molecules to the microtoroid's surface causes changes in its resonance frequency. (c) Block diagram of FLOWER. Resonance frequencies of the microtoroid are first found by applying a 100 Hz triangular waveform voltage signal to the frequency modulation (FM) input port of the laser. Frequency locking experiments are performed by applying a 2 kHz sinusoidal dither signal which generates an error signal. A proportional-integral-derivative (PID) controller enables tracking of the resonance wavelength changes of the microtoroid as particles bind. P= polarizer and OC = 1 × 2 optical coupler. Data is recorded using a 24-bit analog to digital converter. Analysis is performed after data acquisition.

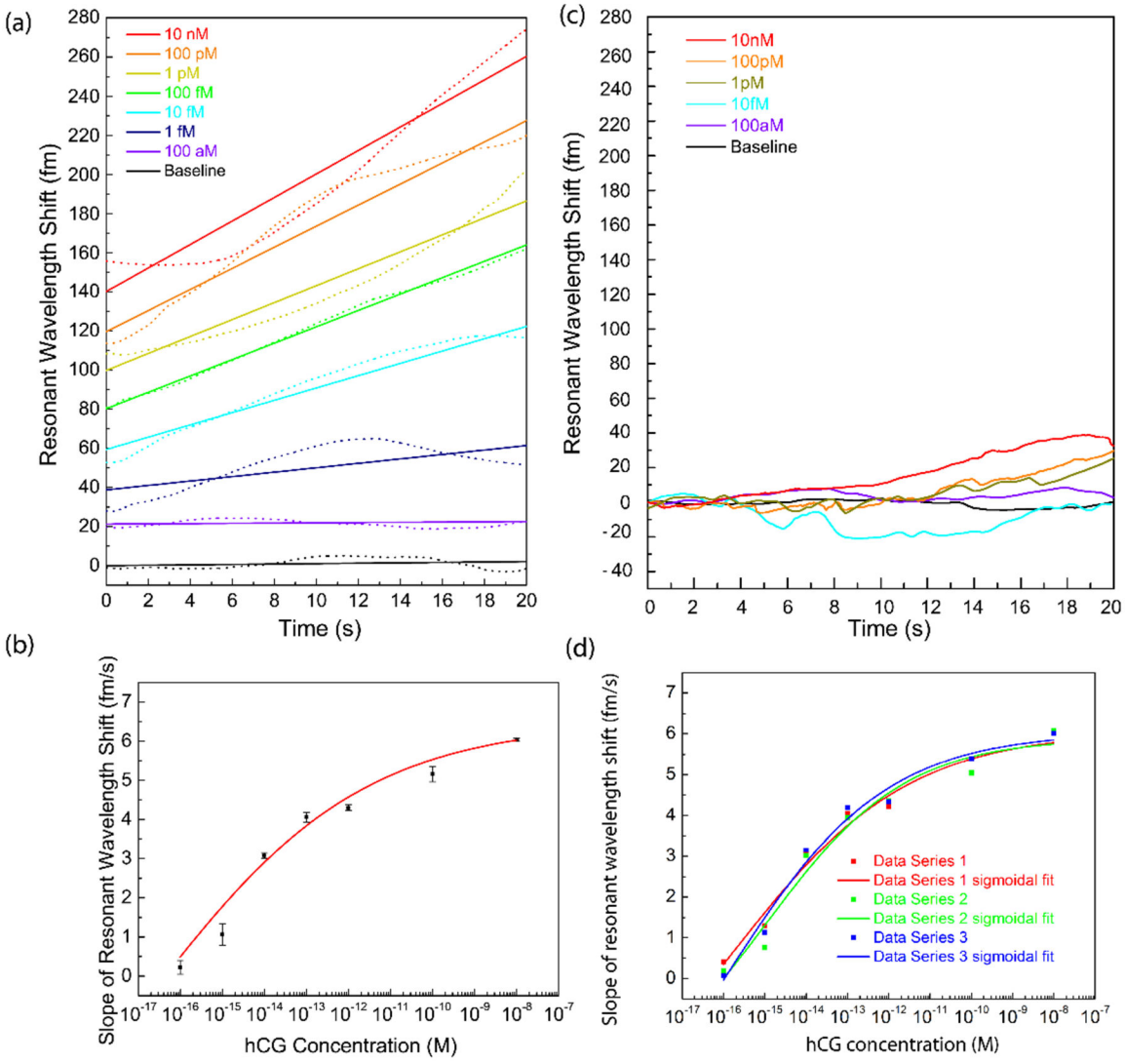

Fig. 2. hCG detection with FLOWER.

(a) Resonant wavelength shifts measured with antibody-functionalized microtoroid biosensors after hCG infusion at different concentrations. Dilutions are prepared in simulated urine. The measurements (dotted lines) were made over 20s. Curves have been vertically separated for clarity. Linear fits are shown as solid lines. The R^2 values of the fits are, in order of high to low concentration: 0.94, 0.947, 0.951, 0.996, 0.974, 0.571, 0.188, 0.079. The variability in the data comes from mechanical fluctuations of the optical fiber used to couple light into the resonator. (b) Binding curve of hCG binding to antibody functionalized microtoroids at different concentrations. The data presented is the average and standard deviation of three independent experiments shown in (d). (c) Binding of hCG to mismatched antibodies bound to the surface of the toroid. Anti-amyloid-β is covalently bound to the surface of the toroid. When hCG is flowed over the surface of our resonator, no concentration dependent increase in binding is observed. Although no surface blocking steps are used, we do not see much nonspecific binding when using the mis-matched antibody. (d) Comparison of hCG detection measurements using three different microtoroids. Three

independent data sets of resonant wavelength shifts, as well as their sigmoidal fits from these measurements are plotted on the same graph to demonstrate the reliability of the microtoroids as biological sensors.

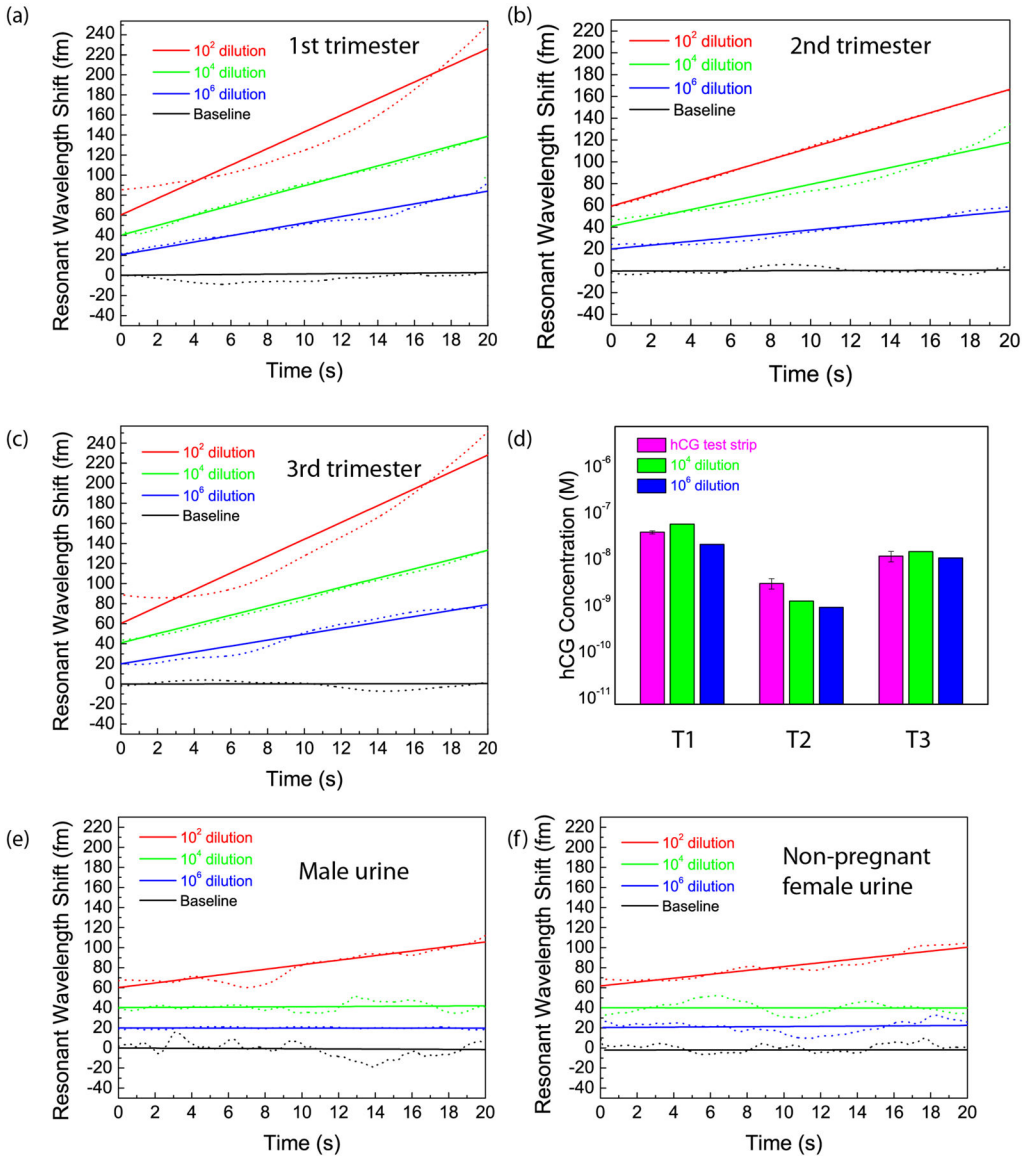

Fig. 3. Ultrasensitive and selective detection of hCG in urine.

a-c, Detection of hCG from the urine of pregnant women during the 1st, 2nd, and 3rd trimesters of pregnancy, respectively. Three different dilutions in simulated urine were tested using the same toroid. The amounts of hCG in the 10^6 times diluted samples are estimated to be 37 fM, 3 fM, and 11 fM at each trimester. **d**, Comparison of the urine hCG concentrations measured using hCG test strips (magenta) with the measurements of 10^4 times (blue) and 10^6 times (red) diluted urine samples for each trimester (T1, T2, and T3) of pregnancy. This is obtained by correlating the resonant shifts observed with the dose response graph in Fig. 2b. The FLOWER measurement results agree with the values measured using pregnancy test strips. The 10^2 times diluted samples had shifts exceeding the measured detection range, probably due to the effect of non-specific interactions in urine. **e,f**, Detection of hCG from the urine sample from a male and a non-pregnant female donor. Three different dilutions in simulated urine were tested with the same anti-hCG functionalized toroid for each of the

urine samples. The urine hCG concentration is expected to be 120 fM for healthy males, and 150 fM for healthy non-pregnant females. There is no significant resonance wavelength shift at dilutions of 10^4 and 10^6 for both samples. Curves have been vertically shifted for clarity.

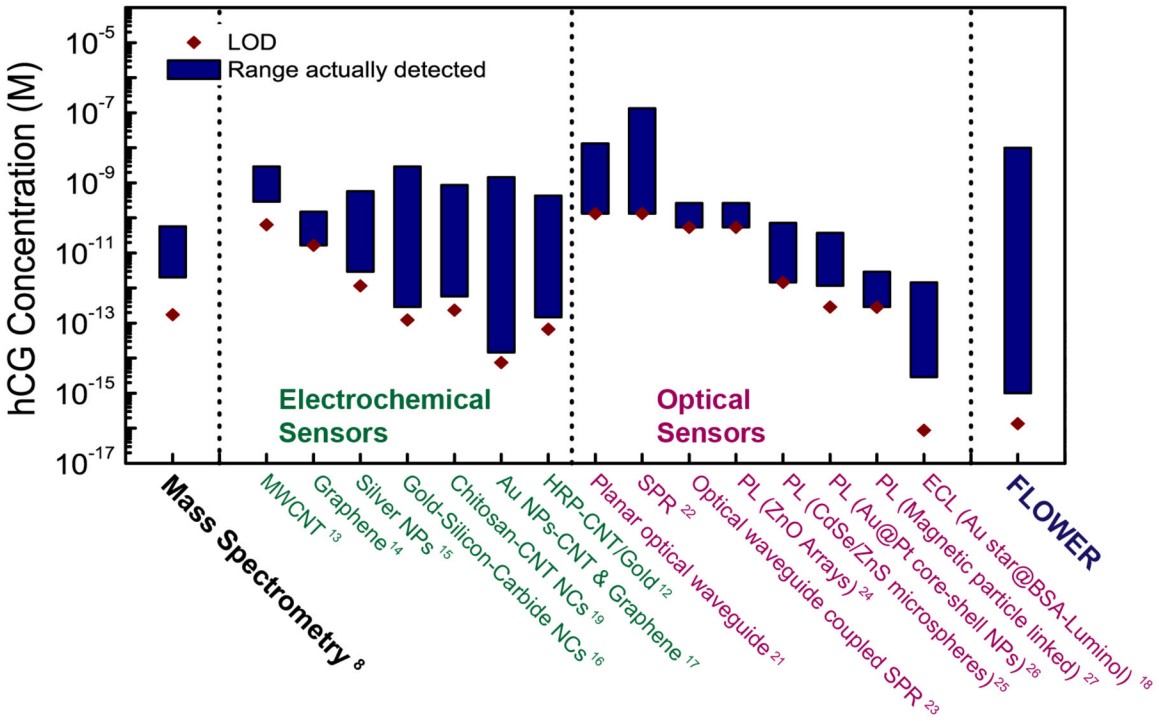

Fig. 4. Comparison of FLOWER with mass spectrometry and other sensors recently demonstrated for hCG detection.

FLOWER is capable of detecting hCG in urine at a concentration three orders of magnitude lower than what has been reported for mass spectrometry. The limit of detection (LOD) of each technique was calculated using the 3σ approach, which is determined by calculating the standard deviation (σ) of several blank samples and multiplying this value by 3. The molar conversion ratio of 2.9 pmol/IU was used to prepare this figure (Stenman, U.H. & Alfthan, H. Determination of human chorionic gonadotropin. *Best Practice & Research. Clinical Endocrinology & Metabolism* **27**, 783–793 (2013).